Int. J. Solids Structures Vol. 30, No. 13, pp. 1777–1788, 1993
Printed in Great Britain

0020–7683/93 $6.00+ .00
© 1993 Pergamon Press Ltd

A FINITE ELEMENT STUDY OF THE TRANSVERSE SHEAR IN HONEYCOMB CORES

M. Grediac
Départment Mécanique et Matériaux, Ecole Nationale Supérieure des Mines de Saint-Etienne, 158, cours Fauriel, 42023 Saint-Etienne Cedex 2, France

(*Received* 5 *July* 1992; *in revised form* 3 *January* 1993)

Abstract—Knowledge of the transverse mechanical properties of honeycomb cores is essential for the design of sandwich panels. This paper deals with the calculation of the transverse shear moduli of a honeycomb sandwich panel by making a finite element study of a representative unit cell. Stress contours inside the honeycomb are also provided. Three cell geometries are studied and the influence of the thickness on the shear modulus and on the homogeneity of the shear stress field is investigated.

NOMENCLATURE

a, t	width, thickness of the inclined wall
b, t'	width, thickness of the central wall
E, G, ν	Young's modulus, shear modulus, Poisson's ratio of the constitutive material
F	loading applied to three adjacent walls
G_{xz}, G_{yz}	transverse shear moduli of the honeycomb
G_{xz}^{higher}, G_{xz}^{lower}	upper and lower bounds for the shear modulus G_{xz}
h	thickness of the honeycomb
R_1, R_2, R_3, R_4	aspect ratios characterizing the unit cell
S	surface of a hexagonal cell
U	horizontal displacement of the top face
u, v	horizontal, vertical displacement of a point located on corner I
α, β	angles involved in the calculation of τ_c
γ_{equ}, τ_{equ}	equivalent shear strain of the honeycomb
γ_c, τ_c	shear strain, shear stress in the central wall
γ_i, τ_i	shear strain, shear stress in the inclined wall
θ	angle cell.

1. INTRODUCTION

Structural sandwich panels with honeycomb core are widespread in aircraft construction and in the building industry because they provide a good compromise between stiffness and lightness. The lightness is due to the core which is bonded to the two thin, stiff and strong skins. The core must also be stiff enough in shear to ensure that when the panel is bent, the two faces of the sandwich panel do not slide over each other. This latter property is mainly related to the transverse shear moduli of the honeycomb. Characterizing these mechanical parameters is therefore an important problem, but a difficult task.

It is easy to show (Gibson and Ashby, 1988), that two different transverse shear moduli characterize the out-of-plane elastic shear behavior of a honeycomb: G_{xz} and G_{yz} (see Fig. 1). Two types of tests can be performed to measure these moduli: a three-point bending test and a rail shear test. However, parasitic effects give rise to some discrepancies between actual and measured moduli (Allen, 1969; Lingaiah and Suryanarayana, 1991). For instance, local bending of the faces or crushing of the core occurs during a three-point bending test. Free boundaries also induce perturbations during the rail shear test.

Another approach is to calculate the stiffnesses of the honeycombs through theoretical considerations on the cellular structure of honeycombs (Kelsey *et al.*, 1958; Gibson *et al.*, 1982; Gibson and Ashby, 1988). Unfortunately, among all the mechanical parameters, the transverse shear moduli are accurately predicted only in some particular cases.

The aim of this paper is to present a method allowing the calculation of the transverse shear moduli of honeycomb cores as well as the state of stress in the walls of the honeycomb. A cell representing the whole network is studied with finite element simulations. The

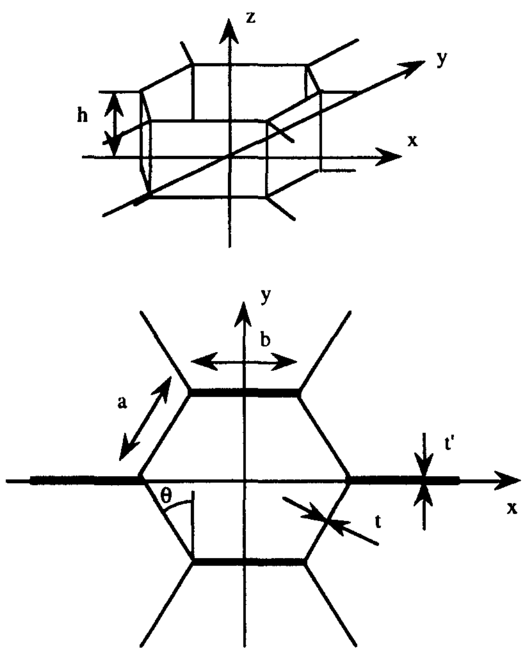

Fig. 1. Geometry of the honeycomb.

choice of the cell as well as the imposed boundary conditions are discussed. Some typical computations of the shear moduli are presented and compared with theoretical results. A formula providing G_{xz} as a function of the aspect ratio of the honeycomb is deduced from these finite element calculations. Stress concentrations in the vicinity of the skins are also indicated.

2. ANALYSIS

2.1. *Calculation of the transverse shear moduli using a theoretical approach*

A honeycomb can be considered as an interconnected network of plates which are the faces of the cells (Fig. 1). This property has been used by Kelsey *et al.* (1958), Penzien and Didriksson (1964) and more recently by Gibson *et al.* (1982) and Gibson and Ashby (1988) who considered the cell deformation under different loadings to provide the honeycomb stiffnesses as functions of its geometry. Some typical properties of these cellular solids, like a negative Poisson's ratio, can be deduced from this approach (Evans, 1991). It must be clearly emphasized that these stiffnesses are calculated assuming a uniform stress distribution in the walls of the structure. Unfortunately, the actual stress field in the walls of a sheared honeycomb is not uniform and remains unknown in the general case. Hence, Kelsey *et al.* (1958) and Gibson *et al.* (1988) only provided lower and upper bounds of the shear modulus in a given direction. Those two bounds are equal in direction y for any geometry of the cell (Fig. 1). They are also equal in any direction for regular hexagonal cells with walls of equal thickness. In this latter case, the honeycomb is equivalent to an isotropic medium in the (x, y) plane whereas it is equivalent to an orthotropic one in all other cases.

The two bounds are obtained using the theorems of minimum potential energy and of minimum complementary energy (Shames, 1973). The first theorem gives an upper bound using a kinematically compatible uniform strain field; the second one gives a lower bound using a statically compatible uniform stress field. The following results are directly quoted from Gibson *et al.* (1988) and Kelsey *et al.* (1958).

Let us consider the part of honeycomb depicted in Fig. 1. It is characterized by four dimensionless aspect ratios:

$$R_1 = \frac{t}{b}, \quad R_2 = \frac{a}{b}, \quad R_3 = \frac{h}{a}, \quad R_4 = \frac{t'}{t}. \tag{1}$$

Two cases are usually considered:

Case 1: $R_4 = 2$. In this case, the honeycomb is built up from metal foil using the corrugated or expansion process (Marshall, 1982). The shear modulus in directions x and y is

$$\frac{1+R_2 \sin\theta}{R_2(1+R_2)\cos\theta} R_1 G \leqslant G_{xz} \leqslant \frac{1+R_2 \sin^2\theta}{(1+R_2 \sin\theta) R_2 \cos\theta} R_1 G, \tag{2}$$

$$G_{yz} = \frac{\cos\theta}{1+R_2 \sin\theta} R_1 G, \tag{3}$$

where G is the shear modulus of the constitutive foil material.

Case 2: $R_4 = 1$. The thickness of the honeycomb is the same in all the walls. The shear modulus in directions x and y is

$$\frac{1+R_2 \sin\theta}{R_2(2+R_2)\cos\theta} R_1 G \leqslant G_{xz} \leqslant \frac{1+2R_2 \sin^2\theta}{2R_2(1+R_2 \sin\theta)\cos\theta} R_1 G, \tag{4}$$

$$G_{yz} = \frac{\cos\theta}{1+R_2 \sin\theta} R_1 G. \tag{5}$$

For walls of equal length (i.e. $R_2 = 1$), the maximum difference between the two bounds of G_{xz} is obtained for $\theta = 0$. Such a cell geometry is obtained with overexpanded honeycombs. Equations (2) and (4) reduce to:

Case 1:

$$\frac{R_1}{2} G \leqslant G_{xz} \leqslant R_1 G; \tag{6}$$

Case 2:

$$\frac{R_1}{3} G \leqslant G_{xz} \leqslant \frac{R_1}{2} G. \tag{7}$$

Using this approach, the shear modulus G_{xz}, which is one of the most important mechanical parameters of honeycombs, is predicted with a maximum uncertainty of 100% in the first case. Such a difference is due to the fact that several assumptions are made to obtain these bounds. It can also be noted that the aspect ratio R_3 is not involved in this theoretical approach. Penzien and Didriksson (1964) considered the influence of the bonding of the honeycomb to the skins to assess its influence on the shear modulus. They have shown under several simplifications that boundary conditions induce warping at the upper and lower faces of the honeycomb and that the lower bound proposed by Kelsey *et al.* (1958) in eqn (2) can be considered as a good estimate of the shear modulus for hexagonal cells with high aspect ratio R_3.

2.2. *Deformation mechanisms in a sheared honeycomb*

The goal here is to describe the deformed shape of a honeycomb whose walls are subjected to pure shear stress. It will be shown that homogeneous stress fields in the walls induce a rotation of the top and the bottom faces of the honeycomb which is not compatible

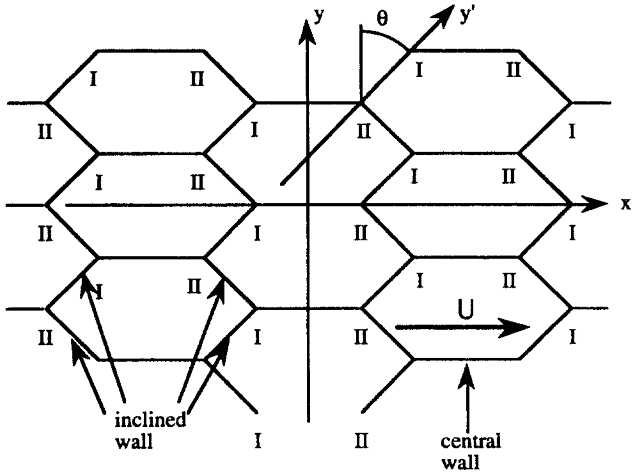

Fig. 2. View of the two types of corners and walls.

with the bonding of the skins. The value of the shear stress in the walls will then be compared to the value of the shear stress obtained with finite element simulations that take into account the bonding of the skins.

Consider a part of a sheared honeycomb depicted in Fig. 2 which is far from the free boundaries. The top face is displaced through a vector U while the bottom face remains fixed. The displacement U is respectively parallel to directions x or y for the determination of G_{xz} or G_{yz}. As G_{yz} is directly given by eqns (3) and (5), only a displacement parallel to direction x is considered here. Two types of walls can be distinguished: inclined walls and central walls. These two types of walls are depicted in Fig. 2. Two types of corners can also be defined: corners I and II. Thanks to the symmetry of the present structure, both of them have the same horizontal displacement. It means that two points $M(x, y, z)$ and $M'(x+b, y, z)$ located respectively on corners I and II have the same horizontal displacement u. On the other hand, their displacements along direction z are unalike (Fig. 3).

The honeycomb is subjected to an equivalent shear strain γ_{equ} defined by

$$\gamma_{\text{equ}} = \frac{U}{h}. \tag{8}$$

The relationship between γ_{equ}, the shear stress and strain in the walls are obtained through simple relations between displacements of corners I and II. Rotations of top and bottom faces of the walls can also be computed as follows.

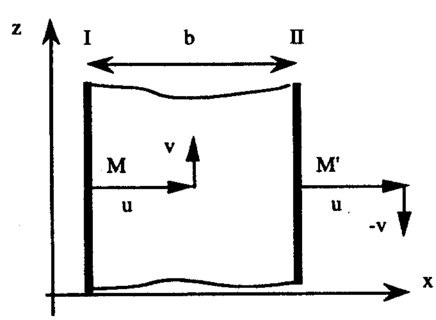

Fig. 3. Displacement of points located on corners I and II.

The top and bottom faces of the central wall rotate through α. Hence, the shear strain in the central wall is [see Fig. 4(a)]

$$\gamma_c = \gamma_{equ} - \alpha \tag{9}$$

with

$$\alpha = 2\frac{v}{b}. \tag{10}$$

The top and bottom faces of the inclined walls rotate through β. Hence, the shear strain in the inclined walls is [see Fig. 4(b)]

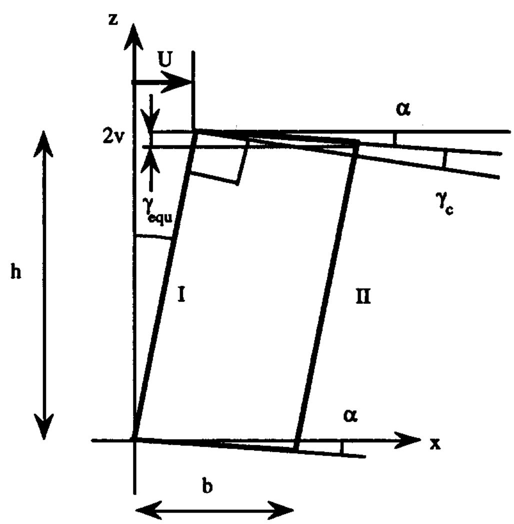

a- central wall in the (x, z) plane

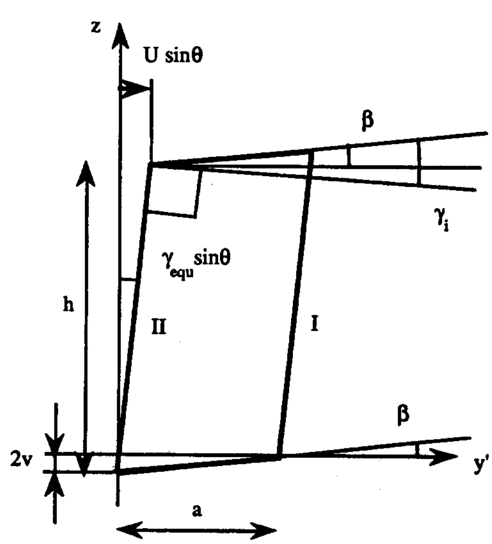

b- inclined wall in the (y', z) plane

Fig. 4. Angles and displacements on the deformed walls.

$$\gamma_i = \beta + \gamma_{\text{equ}} \sin \theta \tag{11}$$

with

$$\beta = 2\frac{v}{a}. \tag{12}$$

Consider here the usual case where $a = b$, one can deduce from eqns (10) and (12) that

$$\alpha = \beta. \tag{13}$$

Let τ_c and τ_i be the shear stress respectively in the central and in the inclined walls. Equilibrium of the corners in direction z gives

$$t'\tau_c = 2t\tau_i. \tag{14}$$

Hence

$$\tau_i = \frac{R_4}{2}\tau_c \tag{15}$$

and

$$\gamma_i = \frac{R_4}{2}\gamma_c. \tag{16}$$

Using eqns (9), (11), (13), (16)

$$\alpha = \frac{R_4 - 2\sin\theta}{R_4 + 2}\gamma_{\text{equ}} \tag{17}$$

and

$$\gamma_i = \frac{R_4\gamma_{\text{equ}}}{(R_4+2)}(1+\sin\theta),$$

$$\gamma_c = \frac{2\gamma_{\text{equ}}}{(R_4+2)}(1+\sin\theta). \tag{18}$$

The shear stress in the walls is finally

$$\tau_i = G\frac{R_4\gamma_{\text{equ}}}{(R_4+2)}(1+\sin\theta),$$

$$\tau_c = G\frac{2\gamma_{\text{equ}}}{(R_4+2)}(1+\sin\theta). \tag{19}$$

Pure shear stress in the walls induces a rotation α of top and bottom faces of the core. This rotation is not compatible with the bonding of the skins. For walls of equal thickness ($R_4 = 1$), one can deduce from eqn (17) that $\alpha = 0$ if $1-2\sin\theta = 0$, that is $\theta = 30°$. Top and bottom faces remain parallel to the skins for regular hexagons with walls of equal thickness. The state of stress is therefore uniform in the walls when the honeycomb is sheared. This is the reason why the two bounds of eqn (4) are equal for $\theta = 30°$.

On the other hand, in the case of honeycombs made from metal foil, $R_4 = 2$ and α cannot be equal to zero when θ lies between 0 and 30°, α is maximum for $\theta = 0°$, i.e. for overexpanded honeycombs. Hence, perturbations in the strain field due to the skin are expected to be the highest for such a cell geometry. That is why the difference between the two bounds of eqn (4) is maximum for $\theta = 0°$.

A better knowledge of the shear stress in the wall is required to predict more precisely the shear modulus G_{xz}. This can be done using a finite element analysis.

2.3. *Description of the process*

Modeling a whole honeycomb for a finite element analysis cannot reasonably be considered because of the complexity of such a structure. The model should have too many degrees of freedom to be studied with usual finite element programs. The method described below allows the calculation of the shear moduli as well as the state of shear stress in the walls of the honeycomb through the study of a very simple model called unit cell which is representative of the whole honeycomb.

The unit cell for the calculation of G_{xz} is depicted in Fig. 5. It is built up with one quarter of one central wall and one quarter of one inclined wall. This reduction in the size of the cell to be studied is due to the different symmetries of the honeycomb. For the calculation of G_{xz}, the top face of the honeycomb is subjected to a uniform displacement U along the x-direction while the bottom face remains fixed. Thanks to the symmetry, the horizontal displacement of the center line CL 1 is $U/2$. Hence, the relative displacement between the top face and CL 1 is $U/2$. The other displacements along the boundary can

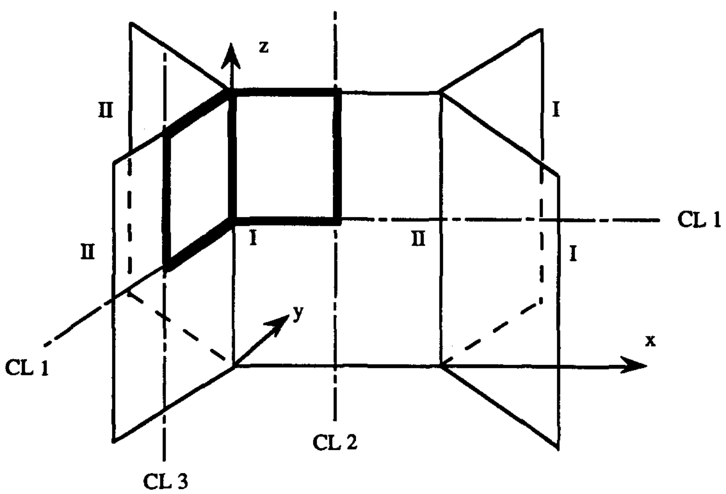

a- center lines on the walls

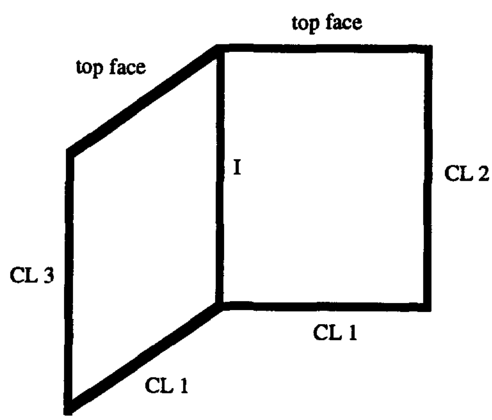

b- unit cell

Fig. 5. Basic cell used for the finite element analysis.

Table 1. Calculation of G_{xz}: Displacements in the global frame along the boundary of the unit cell

	u_x	u_y	u_z
CL 1	R	R	F
CL 2	F	R	R
CL 3	F	F	R
I	F	R	F
top face	$=U/2$	R	R

F: free
R: restrained.

Table 2. Influence of the boundary conditions on the shear modulus G_{xz}, $\theta = 0°$

R_3	G_{xz} Rotations free MPa	G_{xz} Rotations restrained MPa	Relative difference %
1	1840	1910	3.8
1.5	1665	1705	2.3
2	1532	1557	1.6

easily be found with similar considerations. For instance, the vertical displacement along CL 2 and CL 3 is zero; the displacement of corner I along the y-direction is also zero. Note that the thickness of the part of the central wall is divided by 2 thanks to the symmetry of the honeycomb about the x-direction. The displacements along the boundary for the calculation of G_{xz} are reported in Table 1. It must be pointed out that rotations along CL 1, CL 2 and CL 3 are free. On the other hand, rotations along the two lines of the top face can be restrained or free. This point is discussed below. Finally, it must be pointed out that the shear modulus could be computed in any other direction. However, the symmetry about the x-direction could no more be used to reduce the size of the cell to be studied and a cell with two inclined walls would be used.

The equivalent shear modulus is deduced using the following method. As described above, the cell is subjected to an equivalent shear strain γ_{equ}. The force to be applied to shear the unit cell is one quarter of the force to be applied to shear one hexagonal block of equivalent homogeneous material. The equivalent shear stress is computed firstly by adding the magnitude of the forces which have been applied on the top face of the unit cell to obtain the displacement U. The global resulting force is F. The forces on these two lines are necessary to shear one quarter of the hexagon depicted in Fig. 1 which area is

$$S = 2a\cos\theta(b + a\sin\theta). \tag{20}$$

The equivalent shear stress τ_{equ} is then obtained from F and S

$$\tau_{\text{equ}} = \frac{4F}{S}. \tag{21}$$

The equivalent shear modulus G_{xz} is

$$G_{xz} = \frac{\tau_{\text{equ}}}{\gamma_{\text{equ}}}. \tag{22}$$

3. RESULTS AND DISCUSSION

3.1. *Mesh of the unit cell*

Different values of the aspect ratio R_3 between 1 and 10 have been investigated at different angles in order to observe the influence of the core thickness. The other aspect ratios are $R_1 = 0.08$ and $R_2 = 1$. The cell is meshed with 4-noded quadrilateral plate elements formulated in the three-dimensional space. Each node has five degrees of freedom: three translations and two rotations which produce out-of-plane bending. The material characteristics are $E = 72$ GPa and $\nu = 0.31$. The mesh of the walls of the unit cell is such that each wall has four elements along the x-direction. The number of elements along the z-direction is such that the elements have a square shape. It has been checked through a convergence study carried out on a thin cell ($R_3 = 1$; $\theta = 0$) that the present mesh provides a very accurate value of F.

3.2. *Influence of the type of boundary conditions on G_{xz}*

As described above, displacements are restrained on the bottom face and imposed on the top one. The two remaining degrees of freedom, i.e. the two rotations, can be restrained or free. In the first case, the walls are completely embedded. In the second case, they can freely rotate. The reality is between those two cases. The stress in the inclined walls only is influenced by the type of boundary conditions in the case of a displacement along direction x (see Fig. 2). Built-in boundaries induce additional stresses due to bending effect in the areas around the boundaries. Hence, bending effect of the inclined walls is expected to be the highest one in the case of inclined walls perpendicular to the loading direction x ($\theta = 0°$) and for thin honeycombs (low values of R_3). Calculations have been carried out in this case with the two types of boundary conditions. Results are reported in Table 2. As may be seen, the difference between the shear moduli is less than 3.8% and decreases very strongly as R_3 increases. This difference can be considered as negligible and other cell geometries, for which the effect is expected to be smaller, are therefore not studied. All the computations are performed with restrained rotations in the following.

3.3. *Calculation of G_{xz}*

Four cell geometries have been studied: $\theta = 0$, 10, 20 and 30°. Several aspect ratios R_3 between 1 and 10 are considered in each case. The shear moduli G_{xz} computed for these cell geometries are reported in Figs 6–9. Two points are worth noting. Firstly, the difference

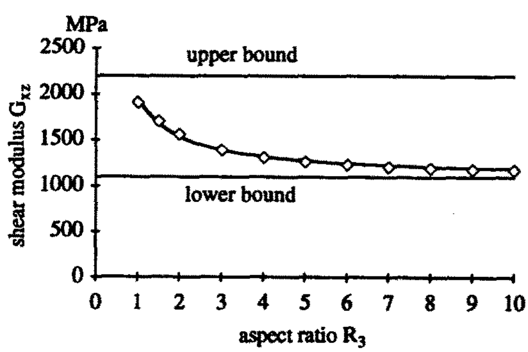

Fig. 6. Shear modulus G_{xz} vs aspect ratio R_3, $\theta = 0°$.

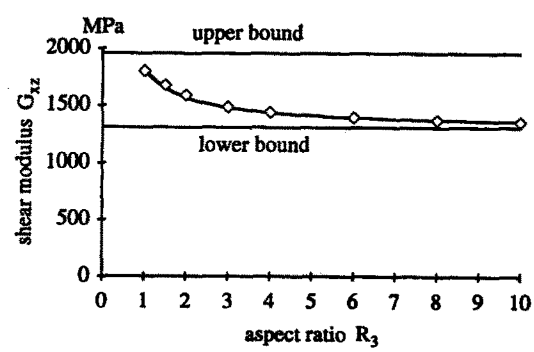

Fig. 7. Shear modulus G_{xz} vs aspect ratio R_3, $\theta = 10°$.

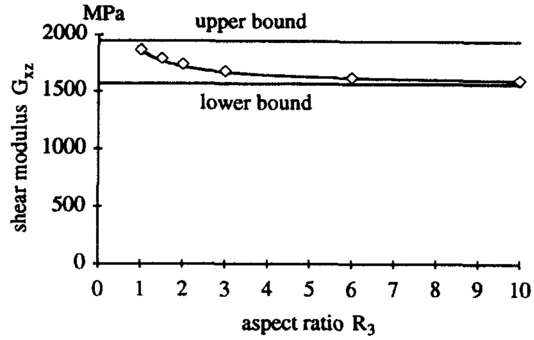

Fig. 8. Shear modulus G_{xz} vs aspect ratio R_3, $\theta = 20°$.

between the two bounds increases as the angle decreases. The shear modulus G_{xz} of over-expanded honeycombs is obtained with a higher uncertainty than for regular hexagonal ones using the approach of Kelsey *et al.* (1958) and Gibson *et al.* (1988). Secondly, G_{xz} decreases as the thickness of the core increases. It can also be noted that these values are in the vicinity of the lower bound. This latter value can therefore be considered as a good estimate of the shear modulus for high aspect ratios. For overexpanded cells ($\theta = 0$), the difference between the shear modulus at $R_3 = 1$ and $R_3 = 10$ is 63%. This difference decreases by 8% for regular hexagonal cells.

3.4. *Shear modulus G_{xz} vs aspect ratio R_3*

Upon further observation of the values computed for these four cell geometries, we note that a relationship of the following type can be used to estimate the shear modulus G_{xz} as a function of the aspect ratio R_3:

$$G_{xz} = G_{xz}^{\text{lower}} + \frac{k}{R_3}(G_{xz}^{\text{higher}} - G_{xz}^{\text{lower}}), \tag{23}$$

where k is a real number, G_{xz}^{higher} and G_{xz}^{lower} are respectively the upper and lower bounds in eqn (2). Constant k has been found using the least squares method with the 30 calculated moduli reported in Figs 6–9: $k = 0.787$. Hence

$$G_{xz} = G_{xz}^{\text{lower}} + \frac{0.787}{R_3}(G_{xz}^{\text{higher}} - G_{xz}^{\text{lower}}) \tag{24}$$

can be considered as a good approximation of the shear modulus for $R_3 \geqslant 1$. This function is plotted in Figs 6–9 and it can be seen that the curves are in agreement with the points

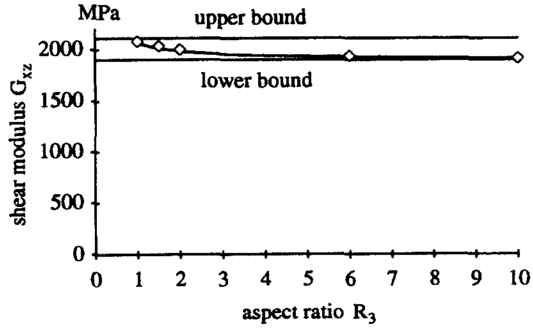

Fig. 9. Shear modulus G_{xz} vs aspect ratio R_3, $\theta = 30°$.

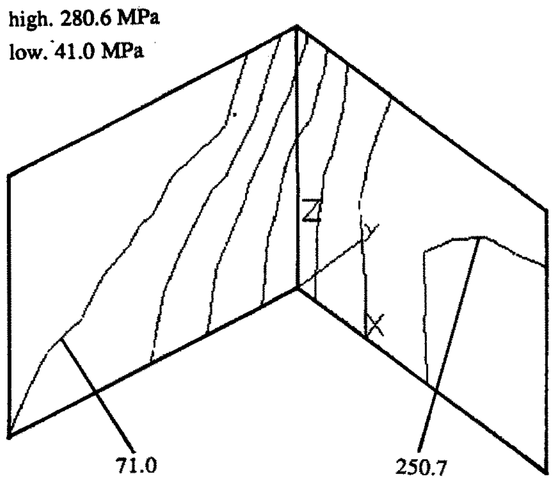

Fig. 10. Shear stress contour, $\theta = 10°$, $R_3 = 1$.

obtained with the finite element calculations. The maximum difference is negligible: 2.7%. It has been obtained for $\theta = 0°$ and $R_3 = 1$.

3.5. *Shear stress contours in the walls*

Figures 10 and 11 show the shear stress contour on the surface of the walls of the unit cell for $\theta = 10°$, $R_3 = 1$ and 6. The relative displacement U between top and bottom faces of the cell is such that

$$\gamma_{equ} = \frac{U}{h} = 10^{-2}. \tag{25}$$

The value of the shear stress can be compared with the shear stress obtained assuming a

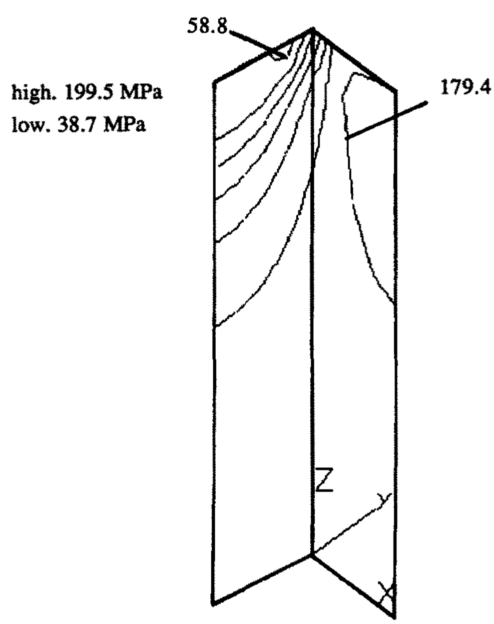

Fig. 11. Shear stress contour, $\theta = 10°$, $R_3 = 6$.

uniform field in the walls using eqn (19). In the present case, $\gamma_{equ} = 10^{-2}$, $\theta = 10°$, $R_4 = 2$ and $G = 27.48$ GPa, the expected value of the uniform shear stress is then

$$\tau_i = \tau_c = 161 \text{ MPa}. \tag{26}$$

As described above, such a shear stress induces shear strain which is not compatible with boundary conditions at both top and bottom faces. The skins induce perturbations in the shear stress field near both top and bottom faces: The shear stress increases in the central wall and it decreases in the inclined wall. This effect cannot be neglected for low values of the aspect ratio R_3. For instance, in the central wall and for $R_3 = 1$ (Fig. 10), the shear stress is 74% higher than in eqn (24). It is 75% lower in the inclined wall. In this case, the shear stress cannot be considered as uniform, even in the middle part of the walls. On the other hand, it is clear in Fig. 11 that the shear stress tends to be uniform in the central part of the walls when the aspect ratio R_3 increases. The perturbation in the stress field also becomes less important in the central wall. For $R_3 = 6$, near the skins, the shear stress increases by 24% in the central wall and decreases by 75% in the inclined wall.

The influence of the skins can be considered as a Saint-Venant effect: simulations performed for higher values of the thickness show that the strain field tends to be uniform in the middle part of the walls as the thickness of the core increases, while it remains heterogeneous near the skins. The shear modulus, which is in fact a global response of this complex structure, depends therefore on the thickness. This effect must be taken into account for the design of sandwich panels with cores characterized by a low R_3 aspect ratio. It must be noted that the measurement of the transverse shear modulus is often carried out on thin cores. The measured values are therefore expected to be higher than the actual shear modulus of thicker cores. The present approach can be used to predict precisely this difference as well as to estimate the stress concentration near the skins and the stress to be carried by the adhesive between honeycomb and skins.

4. CONCLUSION

It has been shown that a suitable choice of a representative unit cell allows the calculation of the transverse modulus as well as of the shear stress contour on the walls of honeycombs. The method has been applied to a set of honeycomb cores and the results are in agreement with theoretical expectations. The influence of the core thickness on the shear modulus G_{xz} is pointed out. A relationship providing this modulus for thin honeycombs is given. The present approach could also be useful for other types of honeycombs built up with shapes of walls different from rectangles, like those described by Marshall (1982), because no theoretical studies have been carried out for such cell shapes.

REFERENCES

Allen, H. G. (1969). *Analysis and Design of Sandwich Panels*. Pergamon Press, Oxford.

Evans, K. E. (1991). The design of doubly curved sandwich panels with honeycomb cores. *Comput. Struct.* **17**, 95–111.

Gibson, L. J. and Ashby, M. F. (1988). *Cellular Solids, Structure and Properties*. Pergamon Press, Oxford.

Gibson, L. J., Ashby, M. F., Schajer, G. S. and Robertson, C. I. (1982). The mechanics of two-dimensional cellular materials. *Proc. R. Soc.* **A382**, 25–42.

Kelsey, S., Gellatly, R. A. and Clark, B. W. (1958). The shear modulus of foil honeycomb core. *Aircraft Engng* 294–302.

Lingaiah, K. and Suryanarayana, B. G. (1991). Strength and stiffness of sandwich beams in bending. *Exp. Mech.*, 1–7.

Marshall, A. (1982). *Sandwich Construction. Handbook of Composites* (Edited by G. Lubin), pp. 557–601. Van Nostrand Reinhold, New York.

Penzien, J. and Didriksson, T. (1964). Effective shear modulus of honeycomb cellular structure. *AIAA Jl* **2**(3), 531–535.

Shames, D. (1973). *Solid Mechanics. A Variational Approach*. McGraw-Hill, New York.